

Mercury in White Sea Bottom Sediments: Distribution, Sources, and Deposition Chronology

Yu. A. Fedorov^{a,*}, A. E. Ovsepyan^a, V. A. Savitsky^a, A. P. Lisitzin^b,
V. P. Shevchenko^b, and A. N. Novigatsky^b

^a*Southern Federal University, Rostov-on-Don, 344006 Russia*

^b*Shirshov Institute of Oceanology, Russian Academy of Sciences, Moscow, 117218 Russia*

**e-mail: fed29@mail.ru*

Received July 10, 2017; revised August 7, 2017

Abstract—For the first time, vertical and lateral distribution patterns of mercury in White Sea bottom sediments have been determined. An abrupt change in the nature of mercury concentrations has been revealed, with a general tendency to decrease with depth. Natural variations in mercury concentrations within 0.01–0.03 µg/g dry weight (dw) have been established. An upper value of 0.03 µg/g dw is taken for the natural background content of the element. The distribution of mercury concentrations in the sequence of bottom sediments is influenced by both anthropogenic and natural factors and processes. With distance from the marine–estuary boundary of the Northern Dvina River, the river’s role in supplying mercury to the White Sea is reduced, and global and regional atmospheric mass transfer take over. The mercury content is used as an indicator of landslide processes in Kandalaksha Gulf of the White Sea. The accumulation chronology of mercury in White Sea sediments is studied, and the proportion of anthropogenic mercury is calculated.

DOI: 10.1134/S0001437019010028

INTRODUCTION

To this day, mercury remains a priority environmental pollutant, of great concern to the global community [20, 21]. When it enters oceans, seas, and lakes, it accumulates in bottom sediments (deposits). V.I. Vernadsky stressed the importance of studying bottom sediments [2]. He considered the surface of the bottom sediments of the World Ocean an extensive boundary between the lithosphere and hydrosphere. Bottom sediments, a relatively open system, are capable of accumulating different substances, including mercury, and a change in the hydrological and biogeochemical conditions at the water–bottom sediment interface may result in its remobilization [21].

Detailed study of bottom sediment cores makes it possible not only to examine the accumulation chronology for various components, but also clarify the background and natural mercury levels for a given object. In turn, knowledge of an element’s background levels makes it possible to calculate the proportion of mercury entering the sea as a result of anthropogenic activity. Humans have utilized mercury since antiquity. Mercury use increased with the onset of the industrial age, which according to various estimates began 250–300 years ago [22]. In addition to the increase in mercury supply into the environment owing to global anthropogenic activity, its supply from regional sources has impacted the White Sea ecosys-

tem. Among the contributors to pollution of the White Sea region are the development of the power industry, industrial production of the Arkhangelsk agglomeration, and the commissioning of the Solombala Pulp and Paper Mill (SPPM) at the end of the 1930s and the Arkhangelsk Pulp and Paper Mill (APPM) at the beginning of the 1950s, which used mercury in the byproduct production cycle.

This study is part of the research program “White Sea Systems” (supervised by A.P. Lisitzin) and the Leading Scientific School (headed by Yu.A. Fedorov) studying the geochemistry of heavy metals, including mercury [3–5, 8–11, 15, 19]. The aim here is to study patterns in the spatial and vertical distribution of mercury concentrations in White Sea bottom sediment cores and to reveal its origin.

MATERIALS AND METHODS

A Niemisto tube was used to sample White Sea bottom sediments on cruise 64 of the R/V *Professor Shtokman* in August 2004 [9]. To study the vertical and spatial distribution of gross mercury in bottom sediments, cores of different thickness were selected from the most representative areas of the White Sea, including Kandalaksha Gulf, the southern and northwestern part of Dvina Bay, and the central and northern areas of the basin (Table 1, Fig. 1).

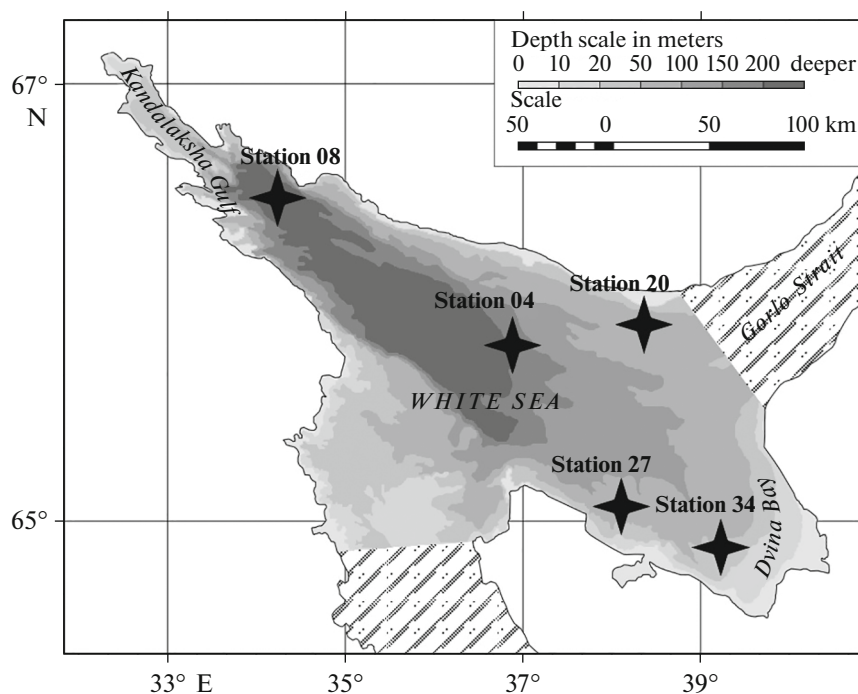


Fig. 1. Location of sampling stations in White Sea.

The bottom sediment sampling depths from the water surface ranged from 40–298 m. The lengths of the cores varied from 14 to 35 cm. The step for determining the gross mercury concentration was 0.5–1.0 cm. The total mercury content was determined by cold vapor atomic absorption at the Geochemical Institute of Roshydromet (analyst A.M. Anikanov). Some 200 determinations were made. All gross mercury concentrations were recalculated to dry weight (dw) and are expressed in $\mu\text{g/g dw}$ [9]. The detection limits

for mercury by the cold vapor atomic absorption method reached 0.0005–0.001 $\mu\text{g/g}$.

Control for repeatable accuracy of the obtained results was carried out at JSC Yuzhgeologia. The determination error was 10–15%. The bottom sediments were dated based on the results from determining the sedimentation rates [18]. Note that calculations employed information from boreholes most closely located to the sampling stations to determine the gross mercury content. For stations 34 and 27, the sedimentation rate was taken as 0.4 mm/yr; for sta-

Table 1. Variations in gross mercury content in White Sea bottom sediments

Station no.	Area	Coordinates, N/E	Mercury content, $\mu\text{g/g dw}$			Standard deviation, $\mu\text{g/g dw}$
			min	mean value	max	
34	Southern part of Dvina Bay	64°50.56' 39°10.23'	0.009	0.019	0.047	0.002
27	Northwestern part of Dvina Bay	65°02.45' 38°00.22'	0.013	0.023	0.035	0.001
20	Basin, Northern part	65°54.20' 38°15.71'	0.012	0.024	0.095	0.006
04	Basin, Central area	65°48.58' 36°45.90'	0.014	0.022	0.050	0.002
08	Kandalaksha Gulf	66°29.10' 34°06.16'	0.006	0.027	0.046	0.003
Entire dataset			0.006	0.023	0.095	0.0028

tions 20, 04, and 08, respectively, the rates were 0.69, 0.85, and 0.46 mm/yr.

RESULTS AND DISCUSSION

The gross mercury content in White Sea bottom sediments varies from 0.006 to 0.095 $\mu\text{g/g dw}$, 0.023 $\mu\text{g/g dw}$ on average. The standard deviation was 0.0028 $\mu\text{g/g dw}$. As well, about 80% of the samples contained less than 0.03 $\mu\text{g/g dw}$ gross mercury. This, as well as the analysis of the gross mercury distribution in geological sections, made it feasible to take this as the background value, which is the upper threshold of its natural content range [9]. For all gross mercury levels below 0.03 $\mu\text{g/g dw}$, the marine ecosystem should be considered insignificantly impacted by anthropogenic activity. Data are available for other areas of the Arctic Basin that indicate background mercury concentrations of 0.02 $\mu\text{g/g dw}$ near the central and western coasts of Greenland and 0.025–0.03 $\mu\text{g/g dw}$ in the eastern part of Hudson Bay [17]. Study [1] is noteworthy, in which for Peter the Great Bay of the Sea of Japan, bottom sediments having gross mercury concentrations of 0.025 $\mu\text{g/g dw}$ have been declared as unpolluted.

Below we discuss the mercury content distribution in vertical sections of bottom sediments for individual stations.

At station 24, sediments were sampled from a depth of 40 m; the sampling depth was 15 cm (Fig. 2a). The mercury content fluctuated from 0.009–0.047 $\mu\text{g/g dw}$, 0.019 $\mu\text{g/g dw}$ on average. Here, for a mercury content decreasing with depth, three peaks of elevated concentration are distinguished at depths of 2, 4, and 10 cm.

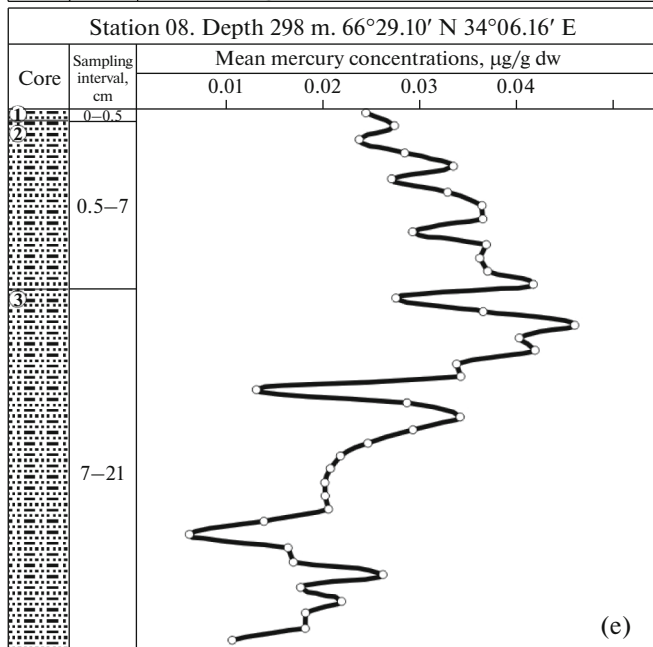
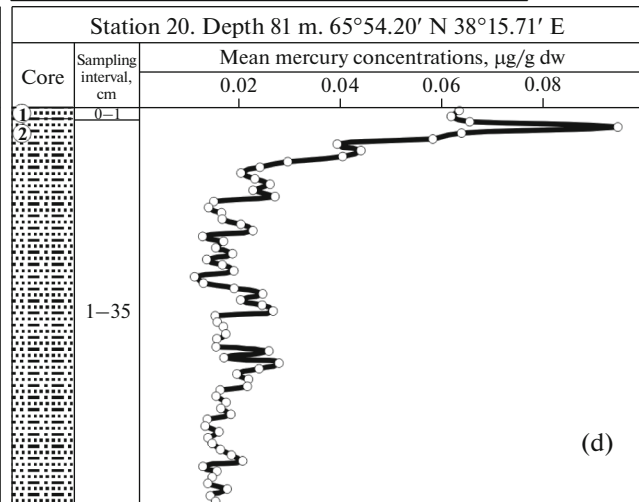
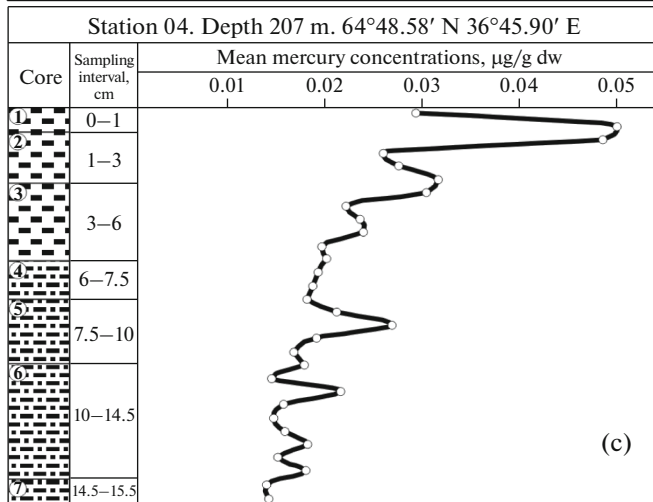
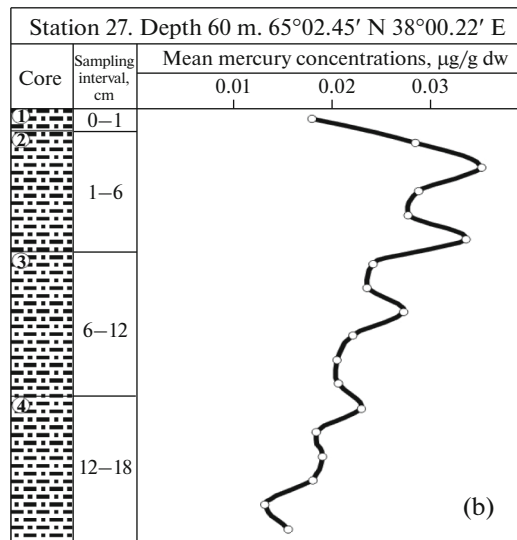
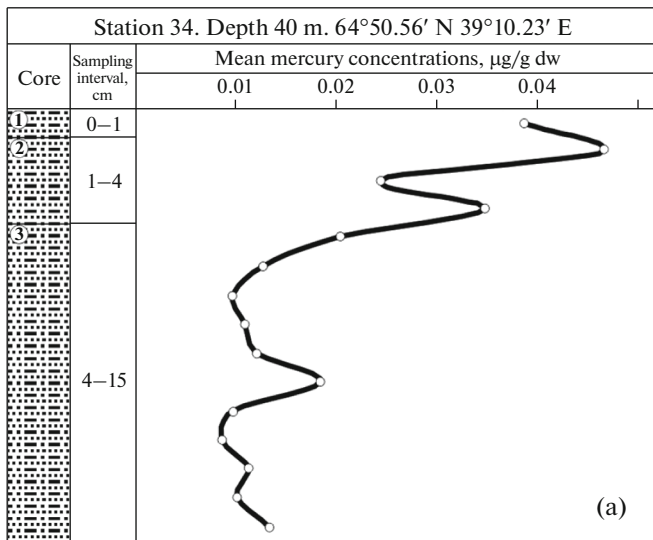
The first, most contrasting peak of the gross mercury content is found in the subsurface layer (at least 2–3 cm thick) of bottom sediments, represented by semifluid sandy-silty deposits. The tip of the peak corresponds to the onset of the active industrialization phase in this area and development of the pulp and paper industry (1930–1960). This time interval also includes military actions associated with WWII. The elevated mercury concentrations during this time can be explained by its entry into bottom sediments mainly via surface runoff from the Northern Dvina River. This is indirectly confirmed by a gross mercury content above its natural background level. To a lesser extent, this may be due to global sources of mercury influx through an atmospheric channel [20, 21]. The second peak is less distinct. Chronologically, it is located higher than the onset of the industrial stage of civilization (about 100 years ago). Its formation may have resulted from global transfer of mercury to Arctic regions, released into the troposphere due to the intensified burning of coal, oil, peat, and as a result of military actions at the front during WWI. The tip of the third peak is related to the onset of industrial

development, but its formation is most likely the result of natural causes. The observed fluctuations in mercury content that do not exceed the natural background level can be considered the result, e.g., of the absence of hydrotroilite and/or organic matter inclusions in the greenish-gray sandy and pelitic-sandy silt.

The sediments at station 27 were sampled from a depth of 60 m; the core length was 18 cm (Fig. 2b). The mercury content ranged from 0.013 to 0.035, averaging 0.023 $\mu\text{g/g dw}$. A spike of elevated gross mercury concentrations was observed at a depth of 2–3 cm. After that, alternating peaks of elevated and lowered mercury concentrations are observed. The composition of bottom sediments here is diverse: in the 0–1 cm interval is a developed thin interlayer of oxidized pelitic sediment, which is replaced (1–6m) first by pelitic silt, and then, toward the sole, by hydrotroilite-rich pelitic silt. The range of natural background values here can be denoted as within 0.015–0.03 $\mu\text{g/g dw}$. Estimating the additive impact of anthropogenic activity (from 1870 to the mid-1990s), let us note that it is distinctly traced in the depth range of 1–5.5 cm and is the result of global-level, regional, and local events. The second peak coincides in time with the onset of the industrial revolution and the California gold rush. The lower-lying detected peaks in gross mercury content to a large extent are related to a natural factor: the presence of hydrotroilite (up to 10% of the sediment volume).

At station 04, bottom sediments were sampled from a depth of 207 m from the 0–15 cm layer (Fig. 2c). The gross mercury concentrations ranged from 0.014–0.05, averaging 0.022 $\mu\text{g/g dw}$. The maximum mercury content is observed at a depth of 2 cm; this spike is dated to the 1980s–1990s. The second peak occurs at a depth of 3–3.5 cm, and its formation can be dated to the 1960s–1970s. It can most likely be assumed that the elevated mercury content formed here under the influence of mercury-contaminated aeolian sediments from an area with pulp and paper production. Downsection, the gross mercury content decreases to a depth of 8.5 cm, where it again somewhat increases (up to 0.027 $\mu\text{g/g dw}$). It is in this horizon that an admixture of hydrotroilite spots is observed, which is a prerequisite for mercury fixation in this layer.

At station 20, sediments were taken from a depth of 81 m; the core thickness was 34.5 m. The gross mercury content ranged from 0.012–0.095, averaging 0.024 $\mu\text{g/g dw}$. (Fig. 2d). The highest gross mercury content (first peak) is found at a depth of 1.5–2 cm, 0.095 $\mu\text{g/g}$ and is the maximum for the entire dataset. This peak is dated to the mid-1970s–1980s. The second peak is less contrastive and is found at a depth of 3.5–4 cm. Its formation corresponds to the mid-1930s–1950s. For a gross mercury content of 0.030 $\mu\text{g/g dw}$ at a sampling depth of 5 cm, a knee is seen in the curve. Further downsection, the mercury content decreases monotonically with depth. The depth distribution of mercury here can be considered



an ideal hyperbolic-type model. Individual mercury content peaks correspond to depths of 7–8, 11, 18, and 22 cm and resulted naturally.

On the whole, analysis of the gross mercury distribution along the sequence of bottom sediments reveals its nonuniformity. A relatively low mercury content is noted in the 0–1.5 cm layer. In the underlying 1.5–2.5 cm layer, a sharp increase in mercury content to maximum values occurs; the minimum values are associated with the bottom layers of the core. Mercury content peaks are also observed in the 7.5–10 cm layer of bottom sediments. It is noteworthy that the station demonstrates the largest difference between the maximum and minimum mercury contents (4.7 times). This station is the farthest from the direct impact of industrial emissions from various enterprises, river runoff, and transport routes; therefore, the main fraction of accumulated mercury influx probably resulted from atmospheric transport during the industrial age, similar to the influx of lead, cadmium, and antimony [14, 20–23]. In addition, this station is located in the northern part of the basin, southwest of the Gorlo Strait. It is well known that more saline waters from the Barents Sea flow along the western shores of the Gorlo Strait into the White Sea Basin [13]. Possibly, the high mercury concentration in the upper sediment horizon resulted precisely from a contact zone of waters here with differing salinity and the accompanying activation of mercury deposition with SPM into bottom sediments. The maximum gross mercury concentration is dated to the 1970s–1980s.

At station 08, sediments were sampled from a depth of 298 m. The thickness of the vertical section was 20.5 cm, and the mercury content here varied between 0.006–0.046 $\mu\text{g/g dw}$, 0.029 $\mu\text{g/g dw}$ on average (Fig. 2d). Here, in contrast to other stations, first, a gradual increase in gross mercury concentrations is noted from the surface to depths of 7.5–10.5 cm, and at a depth of 8.5 cm, it reaches the maximum values. Then, an abrupt reduction in mercury concentrations is seen. The similar character of the change in mercury concentration strongly differs from the other sections. We called this gross mercury distribution along the section “inverted.” This may have resulted from the impact of both natural and anthropogenic factors and processes on bottom sediments. We consider these below.

According to [16], three earthquake activation periods were observed between 1847 and 1995: 1847–1935, 1935–1970, and 1970–1990, which could have led to lateral displacement of bottom sediments from the sides of the bay to its axial part. Landslides may also have been related to frost impacts (frost wedging of sediments and ice cracking in waterbodies). Ice cracking impacted the sides of the bay, which in our opinion could have initiated landslide processes.

Anthropogenic factors in the formation of the inverted section may have been related to construction work in the bay. Thus, analysis of data for 1996–1999 [6], showed that the most polluted areas of the bay are its apices. Back then, construction of a deep channel and expansion of an oil depot were underway, both of which employed explosives. We believe that they may have also led to a change in the current lithological conditions. Redeposition of bottom sediments occurred, a result of which was the shifting of lower horizons to upper ones. Thus, as a result of natural and anthropogenic processes, polluted bottom sediments crept to deeper areas of the bay. Today, they are covered by layers of younger and less polluted bottom sediments.

Our hypotheses are confirmed by contemporary research of the geodynamics of Kandalaksha Gulf of the White Sea [7]. In accordance with the cross section presented in study [7], station 08 is in an active landslide zone. Sediments formed here not only via creeping bottom deposits, but also due to settling of SPM resulting from gravity-related phenomena. Let us attempt to calculate the formation time of a landslide detected from the gross mercury content data.

As mentioned above, the upper boundary of the most polluted bed is at a depth of 7.5 cm. At a sediment formation rate of 0.46 mm/yr in Kandalaksha Bar, it could have been covered by younger sediments in approximately 163 years. However, an increase in the mercury content higher than the background level (0.03 $\mu\text{g/g dw}$) is recorded from a depth of 2.0–2.5 cm. Therefore, it is logical to assume that the top of the landslide is precisely at these depths. Then, the time of its occurrence can be dated to the beginning of the 1950s–1960s. Further down to the bottom of the landslide (at a depth of 15 cm), displaced bottom sediments occur that formed during more significant tectonic events.

Fig. 2. Distribution of gross mercury content in vertical section of White Sea bottom sediments. (a) Station 34. (1) Brown sandy-silt with clay body inclusions; (2) sandy silt, greenish-gray, dense, with rare hydrotroilite inclusions; (3) greenish-gray pelitic-sandy silt. (b) Station 27. (1) pelitic silt, brown, semifluid, sharp lower boundary; (2) pelitic silt, slightly sandy, gray with green hue; (3) hydrotroilite-rich pelitic silt (up to 10% of sediment volume); (4) olive-drab pelitic silt. (c) Station 04. (1) pelitic silt, brown, semifluid, poorly flocculated; (2) pelitic silt, dark brown, semifluid, with elements of thinly veined authigenic inclusions, nonuniform color, lenticular; (3) transition zone, pelitic silt with sand admixture, gray with weak brownish hue, with hydrotroilite in form of black spots, gradual bottom contact; (4) aleuropelite, greenish gray; (5) aleuropelite, gray with greenish hue, with rare hydrotroilite spots; (6) aleuropelite, but more uniform; (7) aleuropelite, gray with greenish hue with distinct hydrotroilite nodules. (d) Station 20. (1) sandy silt, brownish-gray, sediment surface uneven, with dusting of sand, lower boundary quite sharp; (2) sandy silt, gray with greenish hue, texture rough, close to lenticular–laminar, indistinctly expressed spots of organic matter (hydrotroilite). (e) Station 08. (1) thin film of fluid silt, dark brown, flocculated from surface; (2) aleuropelite, brownish gray; (3) aleuropelite, uniform, gray with greenish hue.

Note for all the monitoring stations the presence of relatively lower mercury contents in the uppermost layer, i.e., at the water–bottom sediment interface (0–1 cm). This is because the uppermost layer formed during a reduction in the global and regional influx of mercury into the sea via an atmospheric channel.

Let us analyze the spatial distribution of the gross mercury content in White Sea bottom sediments in terms of horizons. For this, let us calculate the mean content of the metal and its compounds for each station in the 0–5, 5–10, and >10 cm horizons.

The 0–5 cm horizon is characterized by the following variation in the mean concentrations along the profile (Fig. 3). The maximum values were revealed at station 20 (0.057 $\mu\text{g/g dw}$), and the minimum, at station 27 (0.028 $\mu\text{g/g dw}$).

A relatively low mercury concentration is noted in the bottom sediments of Kandalaksha Gulf and the northwestern part of Dvina Bay. The White Sea Basin is characterized by average mercury content values in bottom sediments. The highest values are noted at station 20: 0.03–0.095 $\mu\text{g/g dw}$ (0.057 $\mu\text{g/g dw}$ on average).

In the 5–10 cm horizon, a decrease in the mean mercury content from northwest to southeast is noted. The maximum values were detected at station 08 (0.038 $\mu\text{g/g dw}$), and the minimum, at station 34 (0.013 $\mu\text{g/g dw}$). The lowest mercury contents are characteristic of the southern part of Dvina Bay and the central part of the White Sea Basin; the mean values were detected at stations in the northern part of the basin and the northwestern part of Dvina Bay.

Deeper than 10 cm, the mercury distribution is the most uniform. All of the values are lower than 0.02 $\mu\text{g/g dw}$ and vary from 0.011 $\mu\text{g/g dw}$ (at station 34) to 0.020 (at station 08).

Thus, analysis of the spatial distribution of mercury in the water area of the White Sea demonstrated a nonuniform pattern of variation in the mean mercury content depending on its association with a particular bottom sediment horizon. For the upper horizon (0–5 cm), which is the most indicative of anthropogenic impact, an increased mercury concentration was revealed in contact zones between waters of different origin (Dvina Bay, northern part of the White Sea Basin). For the subsurface horizon (5–10 cm), relatively higher contents are noted in Kandalaksha Bay, which is related to the above-mentioned redeposition of bottom sediments. High concentrations are also preserved at station 20, in the contact zone between White Sea water and water penetrating from the Barents Sea. The underlying horizons (>10 cm) are characterized by relatively low mercury concentrations uniformly distributed over the water area, which formed during civilization's preindustrial period. The jumps in content levels observed at depths of 7.5–10 cm may be related to an increase concentration of iron sulfide here and, as a consequence, complexation and fixation of mercury in these horizons. A similar distribu-

tion is described in the literature [12] and confirmed by a close correlation between the iron sulfide and gross mercury contents in these horizons.

Unfortunately, we were unable to identify the peak mercury contents that form as a result of volcanic eruptions, because volcanic activity has been overshadowed by anthropogenic and natural factors and processes.

Knowing the natural background concentration, let us calculate the proportion of anthropogenic mercury by the formula $C_{\text{fact}} - C_{\text{back}} = C_{\text{anth}}$; $C_{\text{anth}}/C_{\text{fact}} \times 100\% = C_{\text{anth}}, \%$. The largest percentage of anthropogenic mercury is recorded in the 0–5 cm horizon of bottom sediments, where it varies on average from 4% at station 04 to 47% at station 20. In the underlying horizons, the proportion of anthropogenic mercury approaches or equals zero, while only for station 08 is it 20% on average in the 0.5–10 cm horizon. Individual peaks correspond to high levels of gross mercury concentrations, the anthropogenic proportion of which is 68%. The layer of bottom sediments opened at all stations at depths >10 cm (except for station 08) were not impacted by anthropogenic activity, while the mercury levels here should be referred to as natural for the water area of the sea.

CONCLUSIONS

Patterns in the vertical and lateral distributions of the gross mercury content in bottom sediments have been revealed for the first time for the water area of the White Sea. An abrupt character in the change in mercury concentrations was revealed with a general trend toward a decrease with depth. The range of variation of the natural background level of gross mercury concentrations was established (0.01–0.03 $\mu\text{g/g dw}$). The upper threshold of the natural gross mercury concentration range has been substantiated as the background value. All gross mercury content levels less than 0.03 $\mu\text{g/g dw}$ should be considered as having formed under conditions where human activity has not significantly impacted the sea's ecosystem. It has been established that the mercury content in bottom sediments in the water area of the White Sea has a nonuniform distribution. The mean mercury content in bottom sediments of Kandalaksha Gulf is 1.5 times higher than the mercury content in such sediments in the southwestern part of Dvina Bay. The mean concentrations in bottom sediments in the northern part of the sea are somewhat higher. The mean mercury concentrations for the considered bottom sediment horizons at the five studied stations ranges from 0.011 to 0.057 $\mu\text{g/g dw}$. The surface layer is characterized by the following distribution of mean concentrations: maximum, station 20: 0.057 $\mu\text{g/g dw}$; minimum, station 27, 0.028 $\mu\text{g/g dw}$. The chronology of mercury accumulation in White Sea bottom sediments has been studied and its anthropogenic proportion calculated. The mercury concentration distribution along the sec-

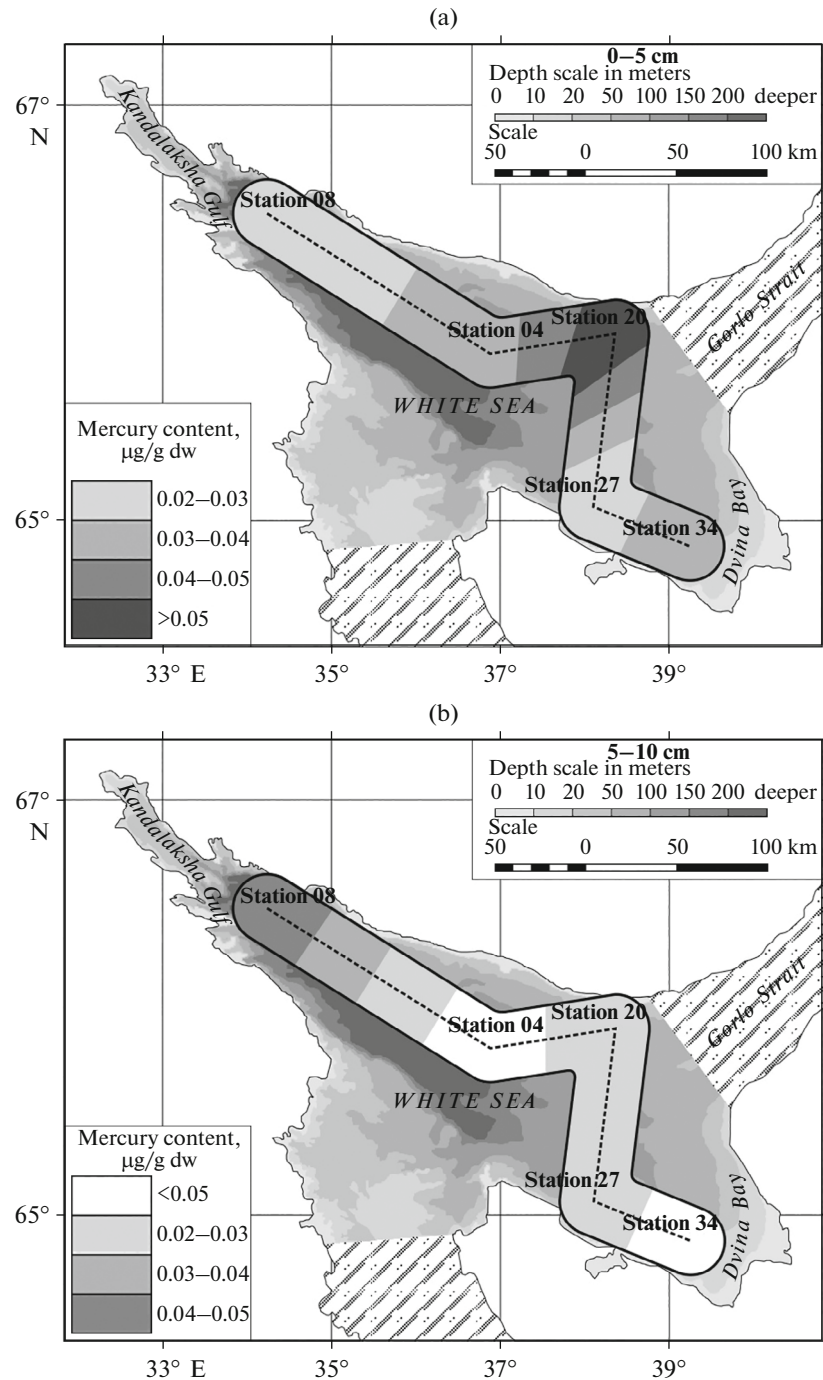


Fig. 3. Distribution of gross mercury content in White Sea bottom sediments. (a) 0–5 cm layer; (b) 5–10 cm layer.

tion of bottom sediments is influenced by both anthropogenic and natural factors and processes. With distance from the mouth region of the Northern Dvina River, its role in mercury transport into the White Sea decreases, and the role of global and regional atmospheric mass transfer of the element increases. The gross mercury content was used as an indicator for the occurrence of landslide processes in Kandalaksha Bay in the White Sea.

ACKNOWLEDGMENTS

The authors thank A.E. Rybalko, D.V. Eroshenko, A.A. Ivanova, and the crew of the R/V *Professor Shtokman* for assistance in sampling.

The study was supported by the following grants: Initiative Science Project (SFU INTERNAL GRANT) no. 5.5795.2017/8.9 and Leading Researchers on a Continuing Basis no. 5.5791.2017/6.7. Interpretation

of the results was supported by the Russian Science Foundation (project no. 14-27-00114-P).

REFERENCES

1. K. I. Aksentov and A. S. Astakhov, "Anthropogenic mercury pollution of bottom sediments of Peter the Great Bay," *Vestn. Dal'nevost. Otd., Ross. Akad. Nauk*, No. 4, 115–121 (2009).
2. V. I. Vernadskii, *Biosphere (Selected Research Works on Biogeochemistry)* (Mysl', Moscow, 1967) [in Russian].
3. L. L. Demina, K. V. Filip'eva, V. P. Shevchenko, et al., "Geochemistry of the bottom sediments in the mixing zone of the Kem' River with the White Sea," *Oceanology* (Engl. Transl.) **45**, 805–818 (2005).
4. G. A. Leonova, V. A. Bobrov, V. P. Shevchenko, and A. A. Prudkovskii, "Comparative analysis of the microelement composition of seston and bottom sediments in the White Sea," *Dokl. Earth Sci.* **406**, 136–140 (2006).
5. A. E. Ovsepyan and Yu. A. Fedorov, *Mercury in the Estuarine Zone of the Northern Dvina River* (Rostizdat, Rostov-on-Don, 2011) [in Russian].
6. V. I. Peresyppkin and E. A. Romankevich, *Biogeochemistry of Lignin* (GEOS, Moscow, 2010) [in Russian].
7. A. E. Rybalko, N. K. Fedorova, M. A. Nikitin, and M. Yu. Tokareva, "Geodynamic processes in Kandalaksha Bay of the White Sea and their role in modern sedimentation," in *Proceedings of XX International Scientific Conference (School) on Marine Geology "Geology of the Seas and Oceans"* (GEOS, Moscow, 2013), Vol. 3, pp. 237–241.
8. *The White Sea System, Vol. 3: Dispersed Sediments of Hydrosphere, Microbial Processes, and Pollution*, Ed. by A. P. Lisitzin and I. A. Nemirovskaya (Nauchnyi Mir, Moscow, 2013) [in Russian].
9. Yu. A. Fedorov, A. E. Ovsepyan, A. P. Lisitzin, I. V. Dotsenko, A. N. Novigatskii, and V. P. Shevchenko, "Patterns of mercury distribution in bottom sediments along the Severnaya Dvina-White Sea section," *Dokl. Earth Sci.* **436**, 51–54 (2011).
10. Yu. A. Fedorov, A. E. Ovsepyan, and V. B. Korobov, "Peculiarities of mercury distribution, migration, and transformation in the estuarine area of the Northern Dvina River," *Russ. Meteorol. Hydrol.* **35**, 289–294 (2010).
11. Yu. A. Fedorov, A. E. Ovsepyan, V. B. Korobov, and I. V. Dotsenko, "Bottom sediments and their role in surface water pollution with mercury (with a special reference to the Northern Dvina River Mouth and the Dvina Bay of the White Sea)," *Russ. Meteorol. Hydrol.* **35**, 611–618 (2010).
12. Yu. A. Fedorov, I. M. Khansivarova, and L. M. Predeina, "Specific distribution of mercury and lead in bottom sediments of Taganrog Bay and the southeastern part of the Sea of Azov," *Vodn. Khoz. Ross.: Probl. Tekhnol., Uprav.* **5** (6), 51–58 (2003).
13. N. N. Filatov and A. Yu. Terzhevik, *The White Sea and Its Watershed Affected by Climate and Anthropogenic Factors* (Karelian Scientific Center, Russian Academy of Sciences, Petrozavodsk, 2007) [in Russian].
14. V. P. Shevchenko, *Impact of Aerosols on Environment and Marine Sedimentation* (Nauka, Moscow, 2006) [in Russian].
15. V. P. Shevchenko, O. S. Pokrovsky, D. P. Starodymova, E. V. Vasyukova, A. P. Lisitzin, S. I. Drovkina, N. S. Zamber, N. M. Makhnovich, A. S. Savvichev, and J. Sonke, "Geochemistry of terricolous lichens in the White Sea catchment area," *Dokl. Earth Sci.* **450**, 514–520 (2013).
16. F. N. Yudakhin and V. I. Frantsuzova, "Seismicity of the White Sea and adjacent areas and its manifestation," in *The White Sea System, Vol. 1: Environment of the Watershed of the White Sea*, Ed. by A. P. Lisitzin, I. A. Nemirovskaya, and V. P. Shevchenko (Nauchnyi Mir, Moscow, 2010), pp. 118–147.
17. *AMAP Assessment 2002: Heavy Metals in the Arctic. Arctic Monitoring and Assessment Program (AMAP)* (Oslo, 2005).
18. R. A. Aliev, V. A. Bobrov, St. N. Kalmykov, et al., "Natural and artificial radionuclides as a tool for sedimentation studies in the Arctic region," *J. Radioanal. Nucl. Chem.* **274** (2), 315–321 (2007).
19. Yu. A. Fedorov and A. E. Ovsepyan, "Mercury and its connection with physicochemical water parameters (case study of the rivers of the Northern European territory of Russia)," in *Mercury: Sources, Applications and Health Impacts* (Nova Science, New York, 2013), pp. 155–172.
20. W. F. Fitzgerald and C. H. Lamborg, "Geochemistry of mercury in the environment," in *Treatise on Geochemistry* (Elsevier, Amsterdam, 2003), Vol. 9, pp. 107–148.
21. W. P. Fitzgerald and R. P. Mason, "The global mercury cycle: oceanic and anthropogenic aspects," in *Global and Regional Mercury Cycles: Sources, Fluxes and Mass Balance*, Nato Science Partnership Subseries 2, Ed. by W. Baeyens, et al. (Springer-Verlag, New York, 1996), Vol. 1, pp. 85–108.
22. P. F. Schuster, D. P. Krabbenhoft, D. L. Naftz, et al., "Atmospheric mercury deposition during the last 270 years: A glacial ice core record of natural and anthropogenic sources," *Environ. Sci. Technol.* **36** (11), 2303–2310 (2002).
23. T. Zalewska, J. Woroń, B. Danowska, and M. Suplińska, "Temporal changes in Hg, Pb, Cd, and Zn environmental concentrations in the southern Baltic Sea sediments dated with ^{210}Pb method," *Oceanologia* **57**, 32–43 (2015).

Translated by A. Carpenter